Open access • Proceedings Article • DOI:10.1117/12.138268

Source localization in a waveguide with unknown large inclusions — Source link

Yongzhi Xu, T. Craig Poling, Trenton J. Brundage

Institutions: University of Minnesota, Alliant Techsystems

Published on: 16 Sep 1992 - Proceedings of SPIE (International Society for Optics and Photonics)

Topics: Point source, Acoustic source localization, Inverse scattering problem, Waveguide and Wave propagation

SOURCE LOCALIZATION IN A WAVEGUIDE WITH UNKNOWN LARGE INCLUSIONS

By

Yongzhi Xu
T. Craig Poling
and
Trent Brundage

IMA Preprint Series # 967
May 1992

Source Localization in a Waveguide with Unknown Large Inclusions

Yongzhi Xu[1]
Institute for Mathematics and its Applications
University of Minnesota
Minneapolis, MN 55455.
T. Craig Poling, Trent Brundage
Alliant Techsystems Inc.
600 Second St. NE
Hopkins, MN 55343

Abstract

In this paper, we combine the matched-field method with the boundary integral equation method from inverse scattering theory to study a sound source localization problem in a shallow ocean with an unknown large inclusion. We assume that there is an unknown inclusion embedded in a shallow water waveguide. To localize a continuous wave (CW) source, we send in a number of "mode waves", which scatter off the unidentified inclusion and are received by a hydrophone array. Combining the information of these scattered waves and the signal from the point source, we present an algorithm to estimate the location of the CW source. A numerical simulation using this method is presented.

1 Introduction

The "Matched-field processing" method for the localization of acoustic sources in waveguides has been studied by many authors in recent years [1] [2] [8] [9] [10]. The main idea of the matched-field processing method is described in Bucker's paper "use of calculated wave field and matched field detection to locate sound source" [2]. On the other hand, the classical inverse scattering theories have developed rapidly recently [3] [11] [5]. The basic idea of the inverse scattering theory is based on the physical idea of scattering one or more "plane waves" off the unidentified inclusion and then trying to identify the shape of the inclusion or other properties from its far-field patterns. Recently, Gilbert and Xu have generalized this idea to the direct and inverse scattering problems in a shallow ocean (ref. [6] [7] [12] [13]).

In this paper, we combine matched-field processing with the boundary integral equation method of inverse scattering theory to study a sound source localization problem in a shallow ocean with an unknown large inclusion. A similar idea has been used by Xu and Yan [15] for sound source localization in a shallow ocean with a known large inclusion. Here we extend the idea to the case that there is an unknown inclusion embedded in a shallow water waveguide. A continuous wave (CW), produced by a sound source, is scattered by the inclusion and then received by a hydrophone array (Figure 1). As we can expect, the existence of the unknown inclusion changes the propagating field greatly. The propagating fields from a point source in a waveguide with and without the inclusion are

[1]This author's research was supported in part by the Institute for Mathematics and its Applications with funds provided by the National Science Foundation, the Minnesota Supercomputer Institute and Alliant Techsystems Inc.

plotted in figures 3 and 4 respectively. Therefore, neglecting the existence of the unknown inclusion will lead to substantial mismatching in the matched-field signal processing.

One straightforward method of avoiding mismatch is to use the inverse scattering method to reconstruct the shape of the unknown inclusion and then use the BIEM method in [14] to estimate the location of the source. However, sometimes one is only interested in locating the sound source. In that case, the method above is not a wise choice because the reconstruction of the unknown inclusion requires a large amount of information and very heavy computation. Moreover, the ill-posedness of the reconstruction problem will cause unnecessary error.

In this paper we will present a method which uses the idea of inverse scattering without actually computing the shape of the unknown inclusion. To localize a continuous wave source we send in a number of "plane waves" which scatter off the unidentified inclusion and are received by a hydrophone array. By combining the information from these scattered waves with the signal from the point source we present an algorithm to estimate the location of the CW source. In Section 2 we formulate the problem and present the theory. Section 3 describes the numerical results.

2 Modeling and methodology

2.1 Modeling

The model of the perturbed waveguide is depicted in figure 1.

We denote the waveguide with depth d as $\mathbf{R}^2_d = \{(x_1, x_2) | -\infty < x_1 < \infty, 0 \leq x_2 \leq d\}$. An inclusion which is a bounded region located in the waveguide is denoted as Ω. For the sake of exposition, we shall assume that the inclusion has a sound-soft boundary $\partial\Omega$. Here we would like to point out that the shape of this inclusion is unknown and no information about Ω is actually used in our computation. A time-harmonic acoustic source is located at $x^s = (x^s_1, x^s_2)$. The hydrophone array consists of L hydrophones at $x^l = (x^l_1, x^l_2), l = 1, 2, \cdots, L$. A time-harmonic wave, radiated from x^s and scattered by Ω, propagates outward to $|x_1| \to \infty$. Let $p(x; x^s)$ be the acoustic pressure at $x = (x_1, x_2)$, emitted from the acoustic source at x^s, and $k = 2\pi f/c$ be the wave number, where f is the frequency and c is the speed of the time-harmonic acoustic wave. If the water waveguide has a pressure release surface at $x_2 = 0$ and a rigid bottom at $x_2 = d$, then the propagation of the outgoing wave is governed by the following equation:

$$\triangle p(x; x^s) + k^2 p(x; x^s) = -\delta(x_1 - x^s_1)\delta(x_2 - x^s_2), \; x = (x_1, x_2) \in \mathbf{R}^2_d \setminus \overline{\Omega}, \tag{2.1}$$

$$p(x_1, 0; x^s) = 0, \quad \frac{\partial p}{\partial x_2}(x_1, d; x^s) = 0, \tag{2.2}$$

$$p(x; x^s) = 0 \text{ for } x \in \partial\Omega. \tag{2.3}$$

Moreover, $p(x; x^s)$ satisfies an outgoing radiating condition, i.e., for $|x_1| \to \infty$, $p(x; x^s)$ has an expansion

$$p(x_1, x_2) = \sum_{n=1}^{\infty} p_n \phi_n(x_2) e^{ik_n|x_1|}, \tag{2.4}$$

where $k_n = [k^2 - (n - \frac{1}{2})^2 \frac{\pi^2}{d^2}]^{1/2}$ is the horizontal wavenumber, and the coefficients p_n depend on x^s and the sign of x_1, and

$$\phi_n(x_2) = \sin[(n - \frac{1}{2})\frac{\pi}{d}x_2]. \tag{2.5}$$

Now we can state our source localization problem as follows: given the acoustic pressure at points $x^l, l = 1, 2, \cdots, L$ in the perturbed waveguide, estimate the location of the sound source x^s.

2.2 Representation of the propagator

In this section we represent the propagating field using the boundary integral equation method on $\partial\Omega$. The purpose is to understand the information that is needed to approximate the propagating field. The integral is defined over an unknown boundary and cannot actually be calculated.

The propagating acoustic wave emitted from a point source at x^s (which is called the *Green's function*) can be constructed in the following way.

Write the Green's function in the waveguide with an inclusion Ω as

$$p(x; x^s) = p_0(x; x^s) + p_1(x; x^s). \tag{2.6}$$

Here $p_0(x; x^s)$ is the Green's function in the waveguide without the inclusion, i.e., $p_0(x; x^s)$ satisfies

$$\triangle\, p_0(x; x^s) + k^2 p_0(x; x^s) = -\delta(x_1 - x_1^s)\delta(x_2 - x_2^s),\ x = (x_1, x_2) \in \mathbf{R}_d^2 \tag{2.7}$$

$$p_0(x_1, 0; x^s) = 0, \quad \frac{\partial p_0}{\partial x_2}(x_1, d; x^s) = 0, \tag{2.8}$$

and $p_0(x; x^s)$ is outgoing. By separation of variables, we can represent $p_0(x; x^s)$ as

$$p_0(x; x^s) = \sum_{n=1}^{\infty} \left\{\frac{i}{2k_n}\right\} \phi_n(x_2)\phi_n(x_2^s) e^{ik_n|x_1 - x_1^s|}. \tag{2.9}$$

Then $p_1 = p - p_0$ is a solution of the problem

$$\triangle\, p_1(x; x^s) + k^2 p_1(x; x^s) = 0,\ x \in \mathbf{R}_d^2 \setminus \overline{\Omega}, \tag{2.10}$$

$$p_1(x_1, 0; x^s) = 0, \quad \frac{\partial p_1}{\partial x_2}(x_1, d; x^s) = 0, \tag{2.11}$$

$$p_1(x; x^s) = -p_0(x; x^s) \text{ for } x \in \partial\Omega, \tag{2.12}$$

and $p_1(x; x^s)$ is out-going as $|x_1| \to \infty$. The physical meaning of this problem is that a wave p_0 incident upon the inclusion Ω produces the scattered wave p_1. The Green's function p is the composition of the incident wave p_0 and the scattered wave p_1.

We construct the scattered wave p_1 by the boundary integral equation method. Using a double layer potential,[4] we write

$$p_1(x; x^s) = \int_{\partial\Omega} \frac{\partial p_0(x; y)}{\partial \nu_y} \psi(y; x^s) d\sigma_y, \text{ for } x \in \mathbf{R}_d^2 \setminus \overline{\Omega}, \tag{2.13}$$

where ψ is the solution of the boundary integral equation

$$\psi(x;x^s) + 2\int_{\partial\Omega} \frac{\partial p_0}{\partial \nu_y}(x;y)\psi(y;x^s)d\sigma_y = -2p_0(x,x^s), \text{ for } x \in \partial\Omega. \tag{2.14}$$

Symbolically we denote the boundary integral equation (2.14) as

$$\psi + \mathbf{K}\psi = -2p_0, \tag{2.15}$$

where $\mathbf{K}$ is the integral operator

$$\mathbf{K}\psi(x;x^s) := 2\int_{\partial\Omega} \frac{\partial p_0}{\partial \nu_y}(x;y)\psi(y;x^s)d\sigma_y, \text{ for } x \in \partial\Omega. \tag{2.16}$$

By the theory of Fredholm integral equations of the second kind, if k is not an eigenvalue of the interior Neumann problem in Ω, then $\mathbf{I}+\mathbf{K}$ is invertible [4]. We can write

$$\psi(x;x^s) = -2(\mathbf{I}+\mathbf{K})^{-1}p_0(x;x^s), \tag{2.17}$$

and

$$p(x;x^s) = p_0(x;x^s) - 2\int_{\partial\Omega} \frac{\partial p_0(x;y)}{\partial \nu_y}(\mathbf{I}+\mathbf{K})^{-1}p_0(y;x^s)d\sigma_y, \text{ for } x \in \mathbf{R}^2_d \setminus \overline{\Omega}. \tag{2.18}$$

2.3 Approximation of the Green's function using the inverse scattering method

The representation (2.18) in the last section cannot be used for computation since Ω is unknown. However, in view of (2.9), we can rewrite (2.18) for $x_1^s < y_1 < x_1$ as

$$p(x;x^s) = \sum_{n=1}^{\infty} \frac{i}{2k_n}\phi_n(x_2^s)e^{-ik_n x_1^s}\left\{\phi_n(x_2)e^{ik_n x_1} - 2\int_{\partial\Omega} \frac{\partial p_0(x;y)}{\partial \nu_y}(\mathbf{I}+\mathbf{K})^{-1}\phi_n(y_2)e^{ik_n y_1}d\sigma_y\right\}. \tag{2.19}$$

For the other cases of x_1^s, y_1, and x_1, we get similar representations by using a proper change of the signs of x_1^s, y_1, and x_1.

Hence, we can approximate $p(x;x^s)$ by

$$p_N(x;x^s) = \sum_{n=1}^{N} \frac{i}{2k_n}u_n(x)\phi_n(x_2^s)e^{-ik_n x_1^s}, \tag{2.20}$$

where

$$u_n(x) = \phi_n(x_2)e^{ik_n x_1} - 2\int_{\partial\Omega} \frac{\partial p_0(x;y)}{\partial \nu_y}(\mathbf{I}+\mathbf{K})^{-1}\phi_n(y_2)e^{ik_n y_1}d\sigma_y, \tag{2.21}$$

and N is the number of propagating modes. If the inclusion Ω is known, (2.21) can be used to calculate u_n, and hence obtain the calculated field. However, since we assume no knowledge of Ω is given, we have to estimate u_n using some other information.

Comparing (2.21) and (2.18), we see that $u_n(x)$ is the sum of the incident wave $u_n^i = \phi_n(x_2)e^{ik_n x_1}$ and the corresponding scattered wave

$$u_n^s = -2\int_{\partial\Omega} \frac{\partial p_0(x;y)}{\partial \nu_y}(\mathbf{I}+\mathbf{K})^{-1}\phi_n(y_2)e^{ik_n y_1}d\sigma_y.$$

That is, an incident "mode wave" u_n^i scatters off the unknown object and produces the scattered wave u_n^s. The total field is the sum of the incident and scattered waves $u_n = u_n^i + u_n^s$.

We compute our estimate of the acoustic field $p_N(x; x^s)$ in two separate steps:

1. Detect $u_n(x^l)$ for given $x^l, l = 1, 2, \cdots, L$. We send in "mode waves" u_n^i for $n = 1, 2, \cdots, N$, and the complex pressures detected at $x^l, l = 1, 2, \cdots, L$ are $u_n(x^l)$.

2. For a given source location x^s, compute $p_N(x^l; x^s)$. After $u_n(x^l)$ are obtained, $p_N(x^l; x^s)$ can be calculated using (2.20).

2.4 Construction of estimators

Using the representations for the Green's function (2.9) and its modal amplitude, we now construct the estimators. For the sake of illustrating our method, we shall use the following simple estimator. More robust estimators will be interesting in practise. However we will not discuss them in this report.

Estimator: Let $\{p_{ml}^*\}$ be the detected data set consisting of the acoustic pressure field p_{ml}^* sampled at the hydrophones located at $(x_1^m, x_2^l), m = 1, 2, \cdots, M; l = 1, 2, \cdots, L$. The estimator in phone space is defined as follows:

$$F_p(x_1^s, x_2^s) = \left[\sum_{l=1}^{L} \sum_{m=1}^{M} \left| p_N(x_1^m, x_2^l; x_1^s, x_2^s) - p_{ml}^* \right|^2 \right]^{-1}, \tag{2.22}$$

where $p_N(x_1^m, x_2^l; x_1^s, x_2^s)$ is the calculated acoustic pressure field at (x_1^m, x_2^l).

3 Computer simulations

Computer simulations using the method above were carried out on the Cray2 at the Minnesota Supercomputer Center. In this section we present some examples from our computations.

Example: Vertical hydrophone array

The configuration for the computer simulations is depicted in figure 2.

We assume the waveguide has a depth of 100 meters. The sound speed is assumed to be $1500m/s$. An acoustic source S located at $(-350/\pi, 100/\pi)$ emits a time-harmonic wave at the frequency $f = 30Hz$. The hydrophone array is arranged vertically at $(600/\pi, 2.5j), j = 0, 1, \cdots, 40$. There is an inclusion Ω with a pressure release surface which occupies the region $\{(x_1, x_2) \mid x_1^2 + 4(x_2 - 50)^2 \leq (50/\pi)^2\}$. If the waveguide is normalized to a depth of π, then the normalized wave number is $k = 4$, which means there are four propagating modes for the acoustic wave at the given frequency.

We use the boundary integral equation method to compute the propagating field. First, we solve the integral equation (2.13) for $\psi(x; x^s)$ where $p_0(x; x^s)$ is given by (2.9) with truncation at $n = 30$ and $x^s = (-350/\pi, 100/\pi)$, and substitute the $\psi(x; x^s)$ into (2.18) to get the propagating field $p(x; x^s)$. A contour plot of the propagating wave with source at $x^s = (-350/\pi, 100/\pi)$ is plotted in figure 3. For comparison, a contour plot of the propagating wave with a source at $x^s = (-350/\pi, 100/\pi)$ in an unperturbed waveguide is plotted in figure 4. In particular, we obtain $p_m^* = p(600/\pi, 2.5m; x^s), m = 0, 1, \cdots, 40$. To make the data more realistic, we add Gaussian noise (generated by a NAG subroutine g05ddf in our computation) to the data and use it as our detected data. Contour plots of the first to

forth modes of the total fields in a waveguide with the large inclusion are given in figures 5-8. For comparison, the forth mode in a unperturbed waveguide is plotted in figure 9.

The second step is to compute the estimator. We generated the $u_n(600/\pi, 2.5m)$ as the detected field at $(600/\pi, 2.5m), m = 0, 1, \cdots, 40$. These data are obtained by our approximate BIEM method with added Gaussian noise.

Using these $u_n(x)$, we search the area of $[-600/\pi, 0.0] \times [0, 100]$, and plot the estimator $F_p(x^s)$ for $x^s \in [-600/\pi, 0.0] \times [0, 100]$. (See figures 10-14).

Figure 10-11: These figures show the estimator $F_p(x^s)$ for the detected data $p_m^* = p(600/\pi, 2.5m; x^s$ $m = 0, 1, \cdots, 40$ which contain Gaussian noise with signal-to-noise ratio $S/N = 10dB$. In figure 11, a filter with the threshold value $F_p(x^s) = 0.65$ is used, i.e. we set $F_p(x^s) = 0$ if $F_p(x^s) < 0.65$.

Figure 12: This figure shows the estimator $F_p(x^s)$ when the calculated field $p_N(x; x^s)$ is computed in the absence of the inclusion and hence mismatches the true field. The figure indicates the processing loss and localization ambiguities incurred by not accounting for unknown inclusions in matched field processing. No noise was used in this calculation.

Figure 13: Same as Figure 15 with added Gaussian noise, signal to noise ratio $S/N = 10dB$, and a filter threshhold value of $F_p(x^s) = 0.65$.

4 Conclusions

A technique for compensating for environmental uncertainty in matched field processing has been described. The method combines the boundary integral equation method with matched field processing. By illuminating the search space with incident "mode waves" the effect of unknown inhomogeneities in the environment on matched field processing can be compensated. The advantages of this compensation on matched field processing gain and localization can be clearly seen by the numerical simulations.

References

[1] Baggeroer, A. B., Kuperman, W. A., and Schmidt, H., "Matched field processing: Source localization in correlated noise as an optimum parameter estimation problem", *J. Acoust. Soc. Am.* 83, 571-587 (1988).

[2] Bucker, H. P., " Use of calculated wave field and matched field detection to locate sound source in shallow water," *J. Acoust. Soc. Am.* 59, 368-373 (1976).

[3] Colton, D., "The inverse scattering problem for time-harmonic acoustic waves", *SIAM Review* 26 (1984) 323-350.

[4] D. Colton and R. Kress, *Integral Equation Methods in Scattering Theory*, John Wiley, New York, 1983.

[5] Colton, D., Ewing, R., and Rundell, W., *Inverse Problem in Partial Differential Equations*, SIAM, Philadelphia, (1990).

[6] Gilbert, R. P. and Xu, Yongzhi, "Starting fields and far fields in ocean acoustics", *Wave Motion*, 11 (1989) 507-524.

[7] Gilbert, R. P. and Xu, Yongzhi, "Dense sets and the projection theorem for acoustic harmonic waves in homogeneous finite depth oceans" *Math. Methods in Appl. Sciences* 12 (1989) 69-76.

[8] Porter, M. B., Dicus, R. L., and Fizell, R. G., "Simulation of matched-field processing in a deep-water Pacific environment", *IEEE OE-12*, 173-181 (1987).

[9] Shang, E. C., Clay, C. S., and Wang, Y. Y., "Passive harmonic source ranging in waveguides by using mode filter", *J. Acoust. Soc. Am.* 78, 172-175 (1985).

[10] Shang, E. C., " An efficient high-resolution method of source localization processing in mode space", *J. Acoust. Soc. Am.* 86 (5) 1960-1964 (1989).

[11] Sleeman, B. D.; "The inverse problem of acoustic scattering", *IMA J. Applied Math.* 29 (1982).

[12] Xu, Yongzhi, "An injective far-field pattern operator and inverse scattering problem in a finite depth ocean", *Proceedings of the Edinburgh Mathematical Society* (1991) 34, 295-311.

[13] Xu, Yongzhi, Poling, T. C., and Brundage, T., "Direct and inverse scattering of time harmonic acoustic waves in inhomogeneous shallow ocean", *IMA Preprint 821*, (1991), to appear in Proceeding of Third IMACS Symposium on Computational Acoustics, Harvard University, 1991.

[14] Xu, Y. and Yan, Y., "An approximate boundary integral equat ion method for acoustic scattering in shallow oceans", to appear in *J. Computational Acoustics*, (1992).

[15] Xu, Y. and Yan, Y., "BIEM for source localization with a CW sonar", to appear in *J. Acous. Soc. Amer.* (1992).

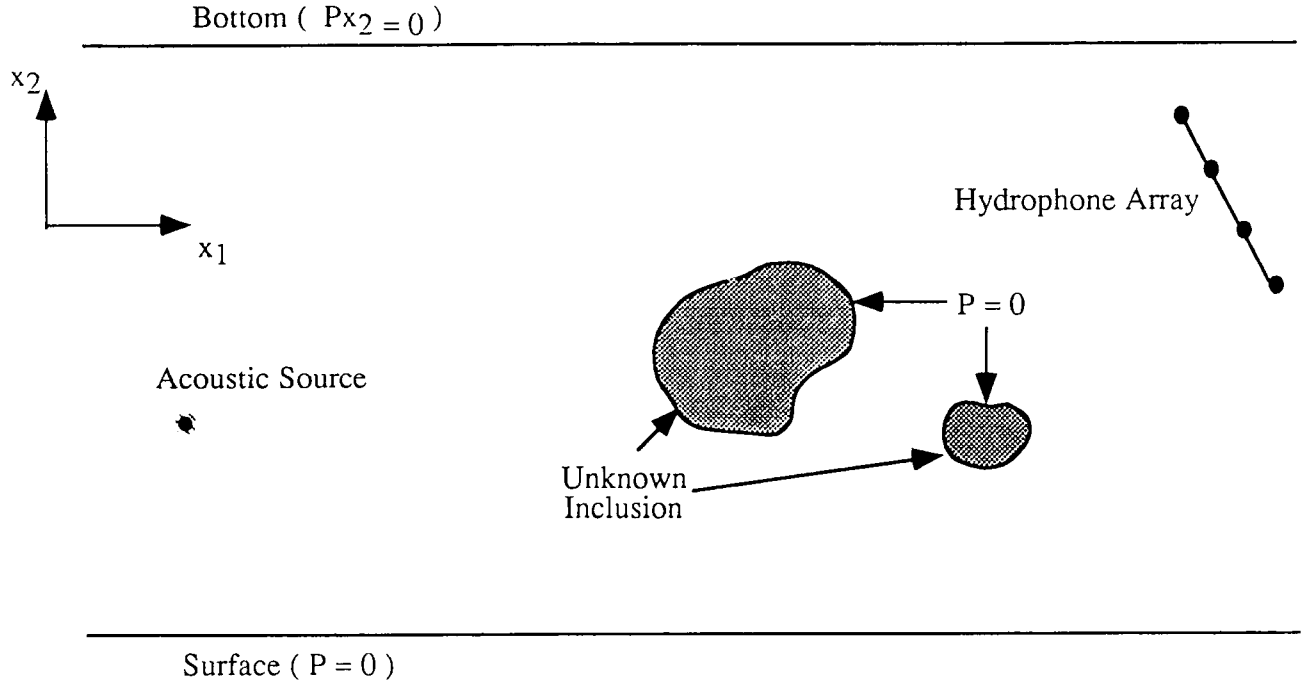

Figure 1: Acoustic source in a perturbed waveguide

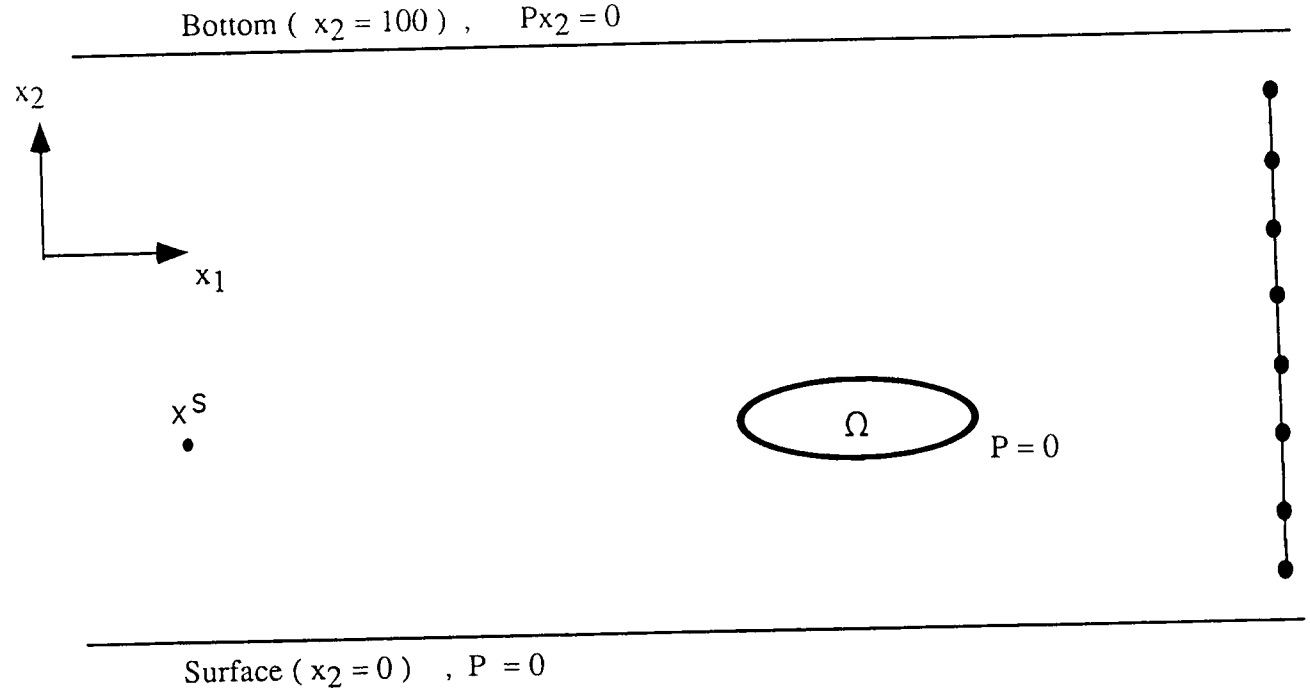

Figure 2: Detection of acoustic source by a vertical hydrophone array

Figure 3: Total propagating wave from the point source in the perturbed waveguide

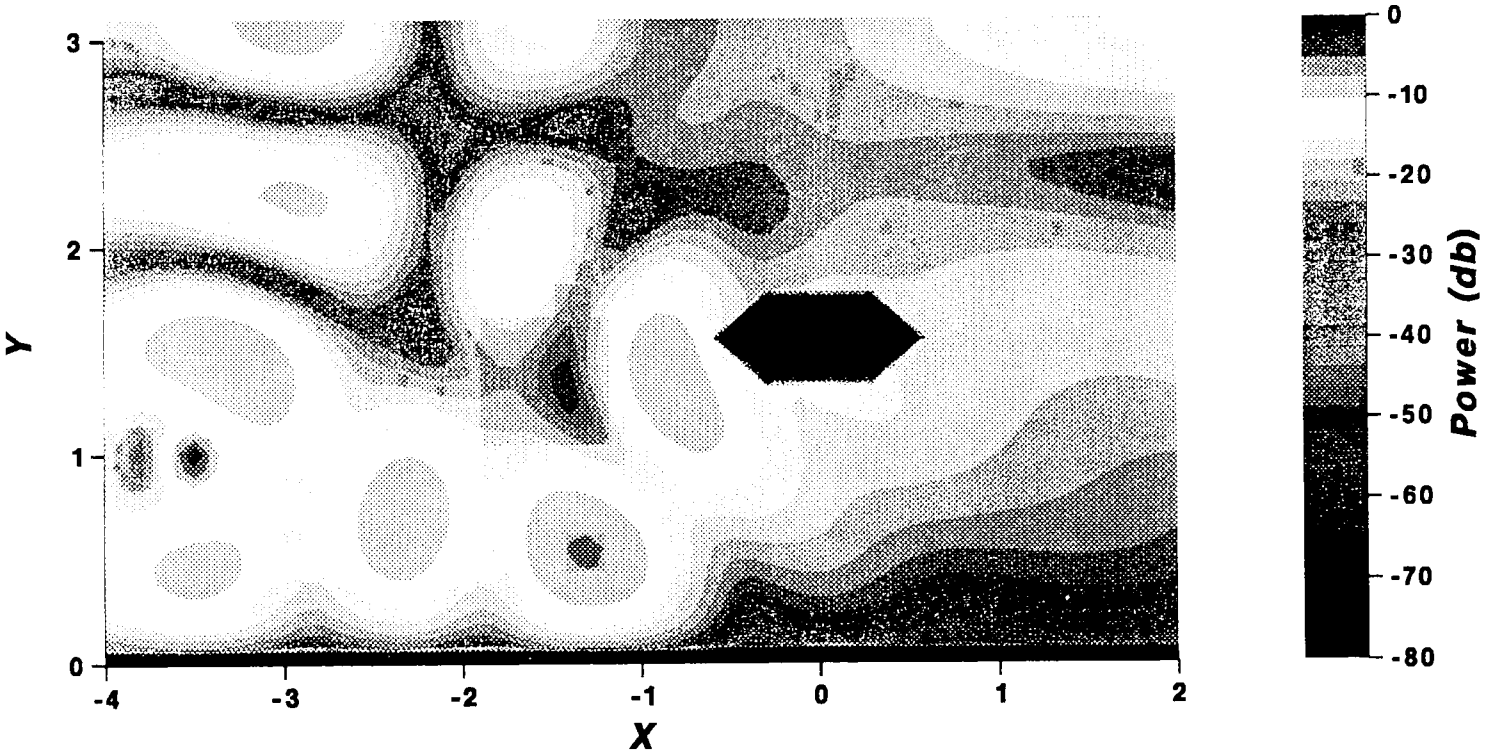

Figure 4: Total propagating wave from the point source in the unperturbed waveguide

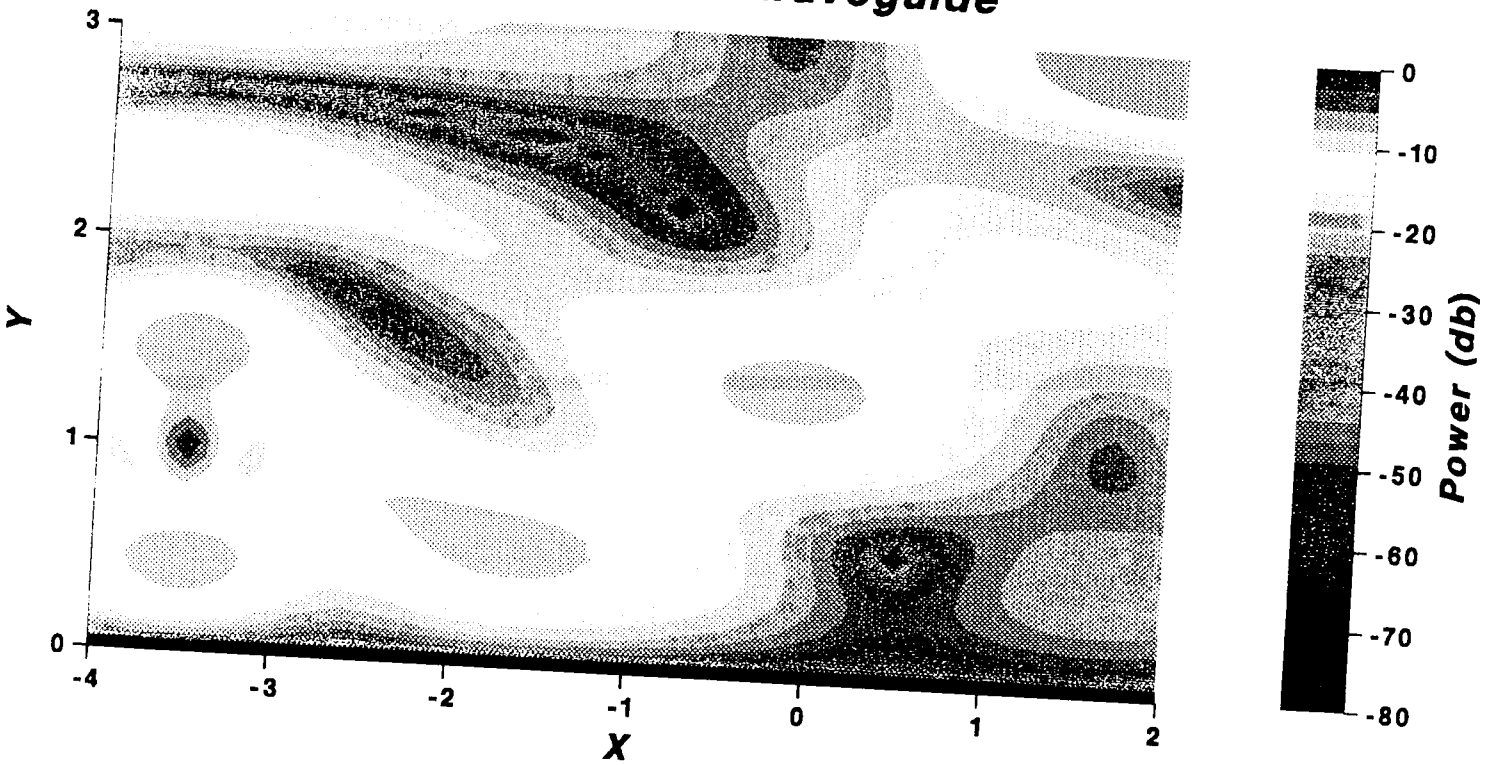

Figure 5: First mode of the total wave in the perturbed waveguide

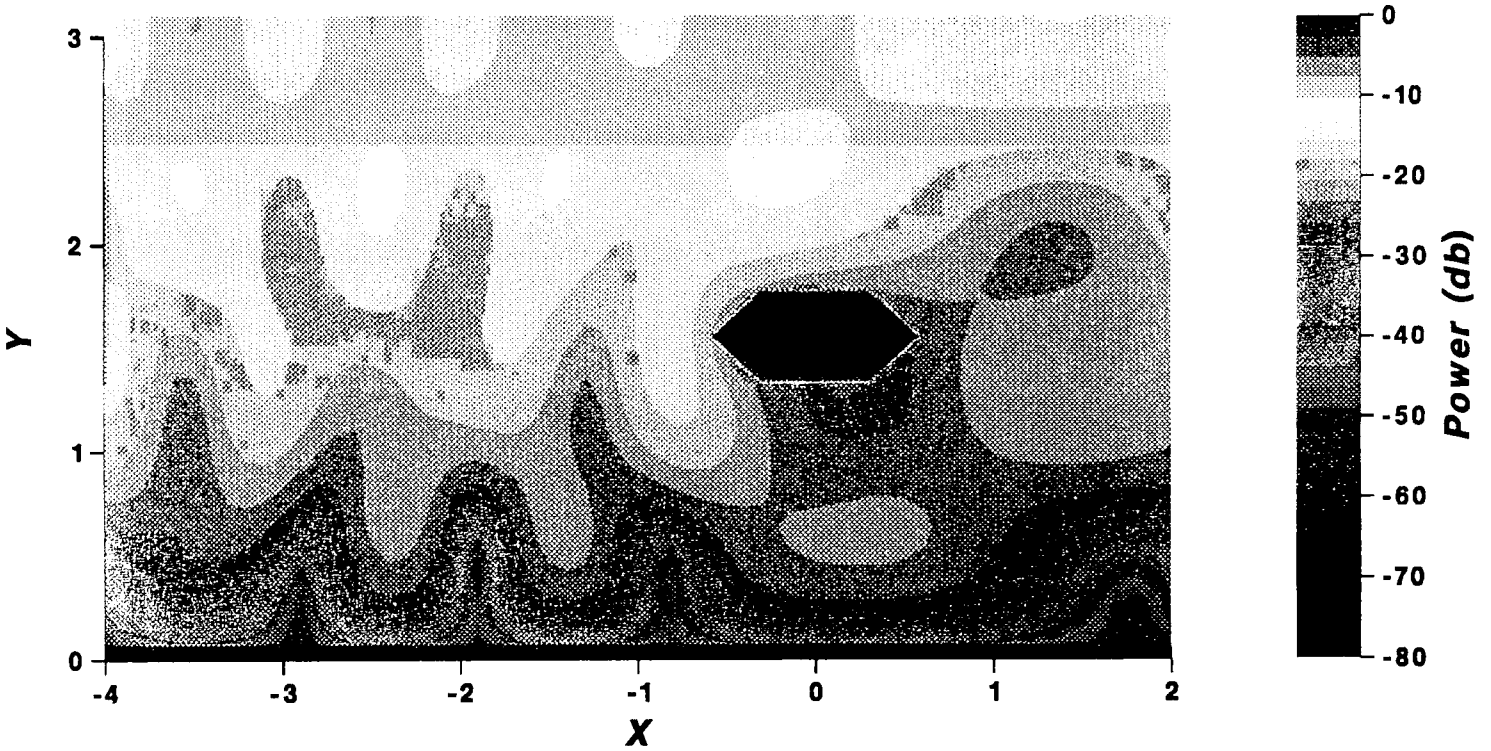

Figure 6: Second mode of the total wave in the perturbed waveguide

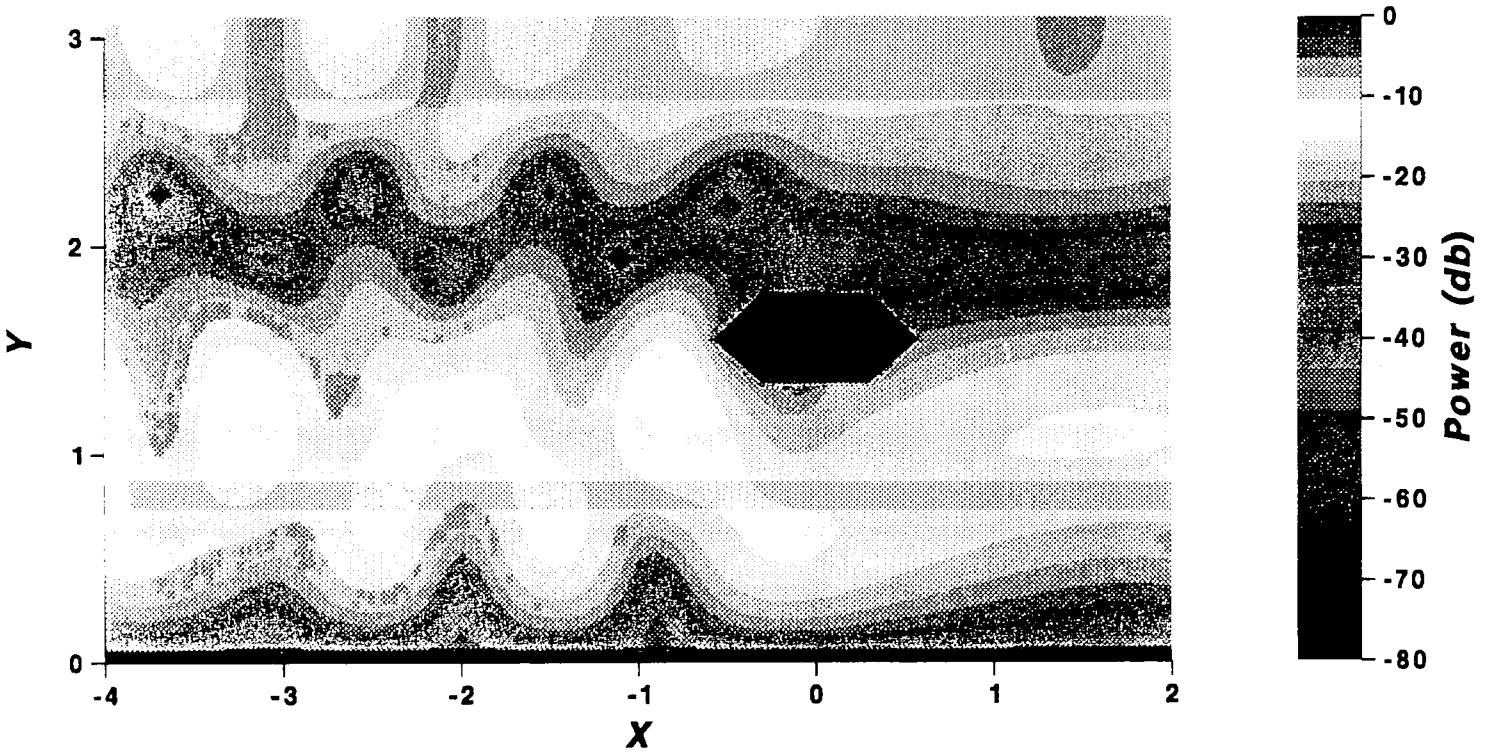

Figure 7: Third mode of the total wave in the perturbed waveguide

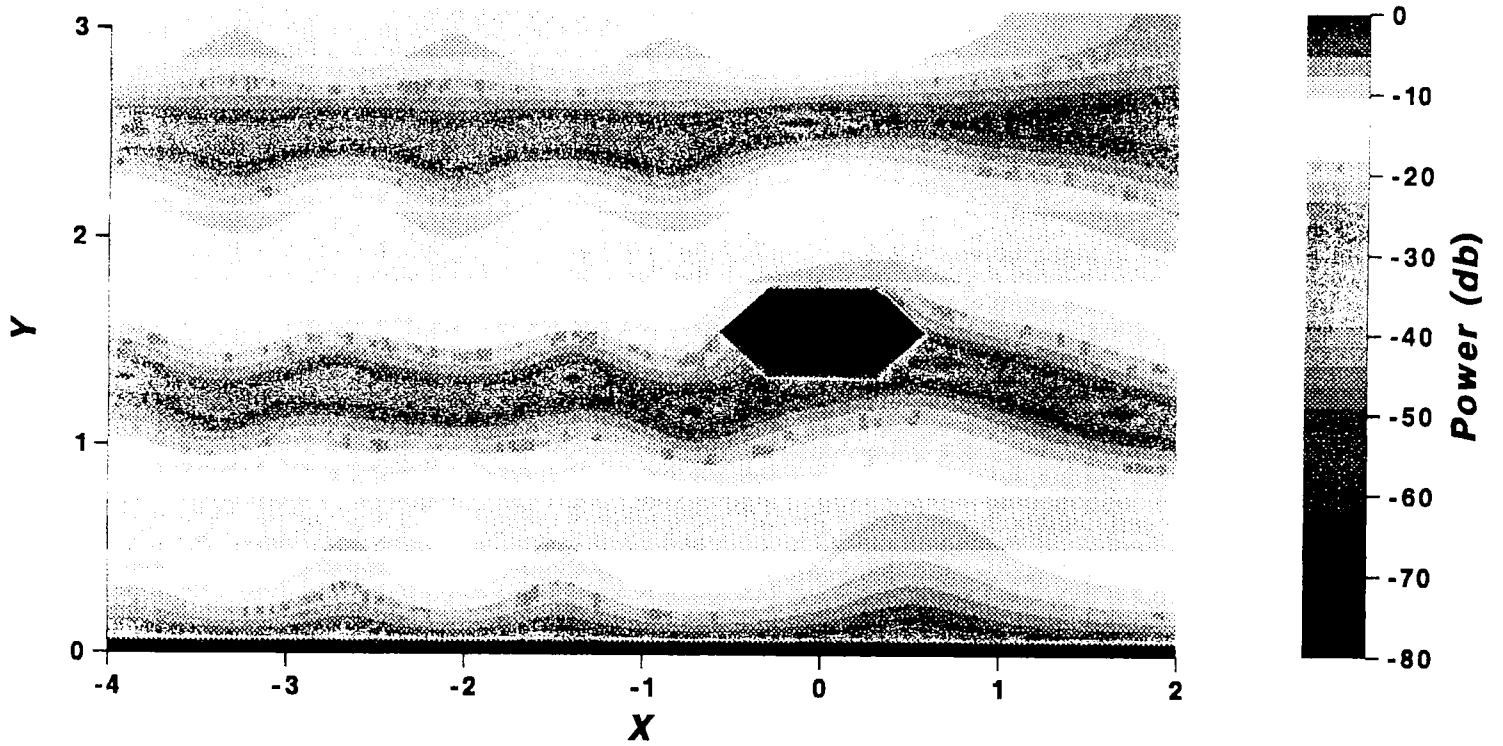

Figure 8: Fourth mode of the total wave in the perturbed waveguide

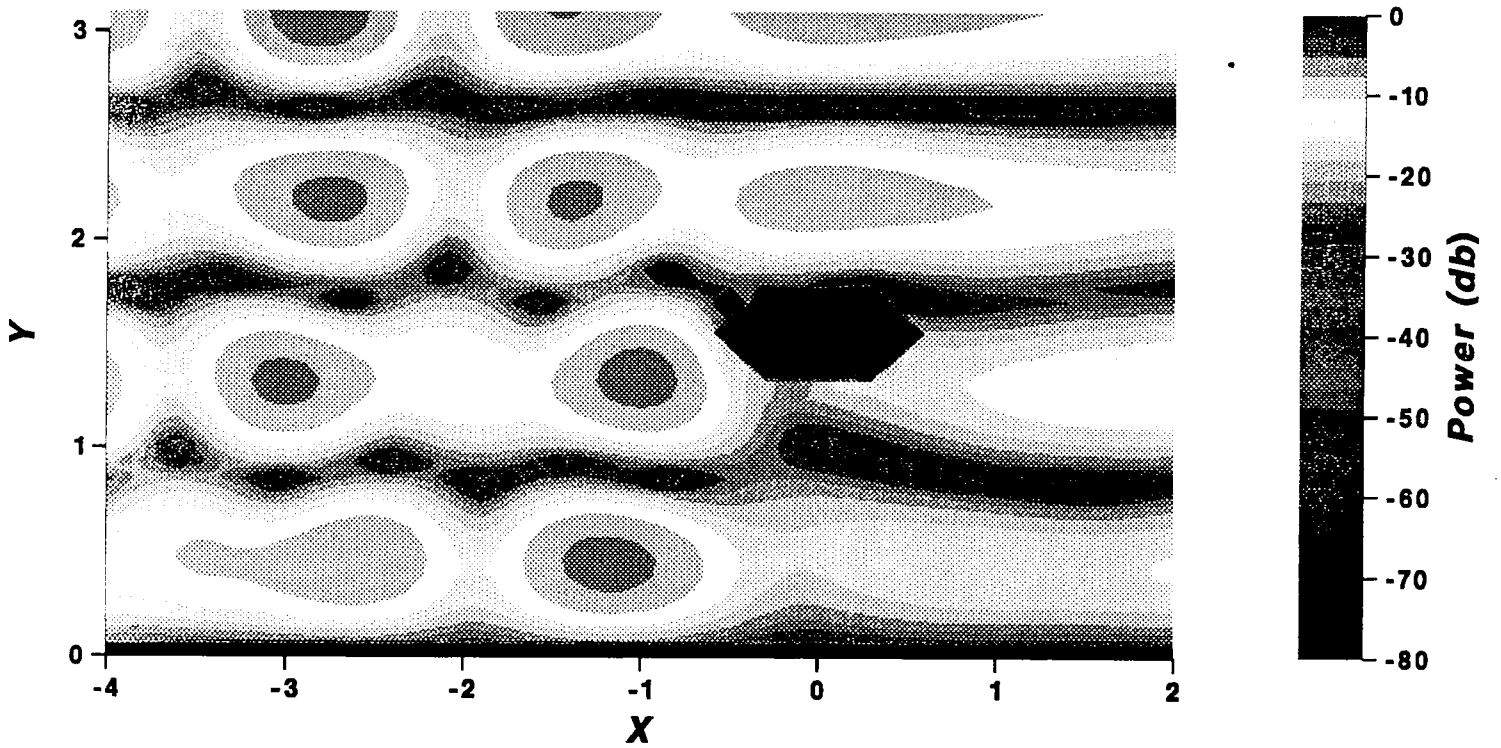

Figure 9: Fourth mode of the total wave in the unperturbed waveguide

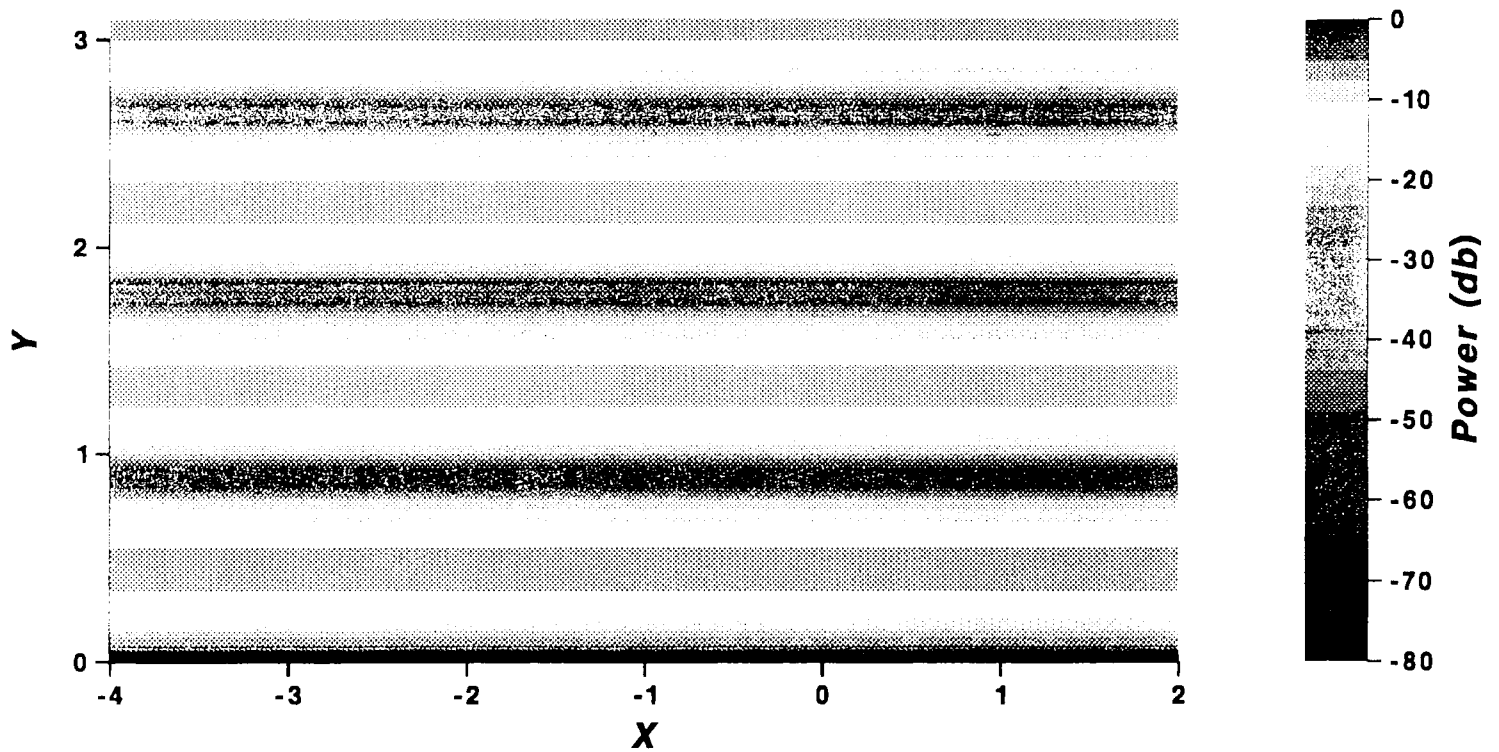

Figure 10: Estimator of detected data with Gaussian noise, S/N=10db

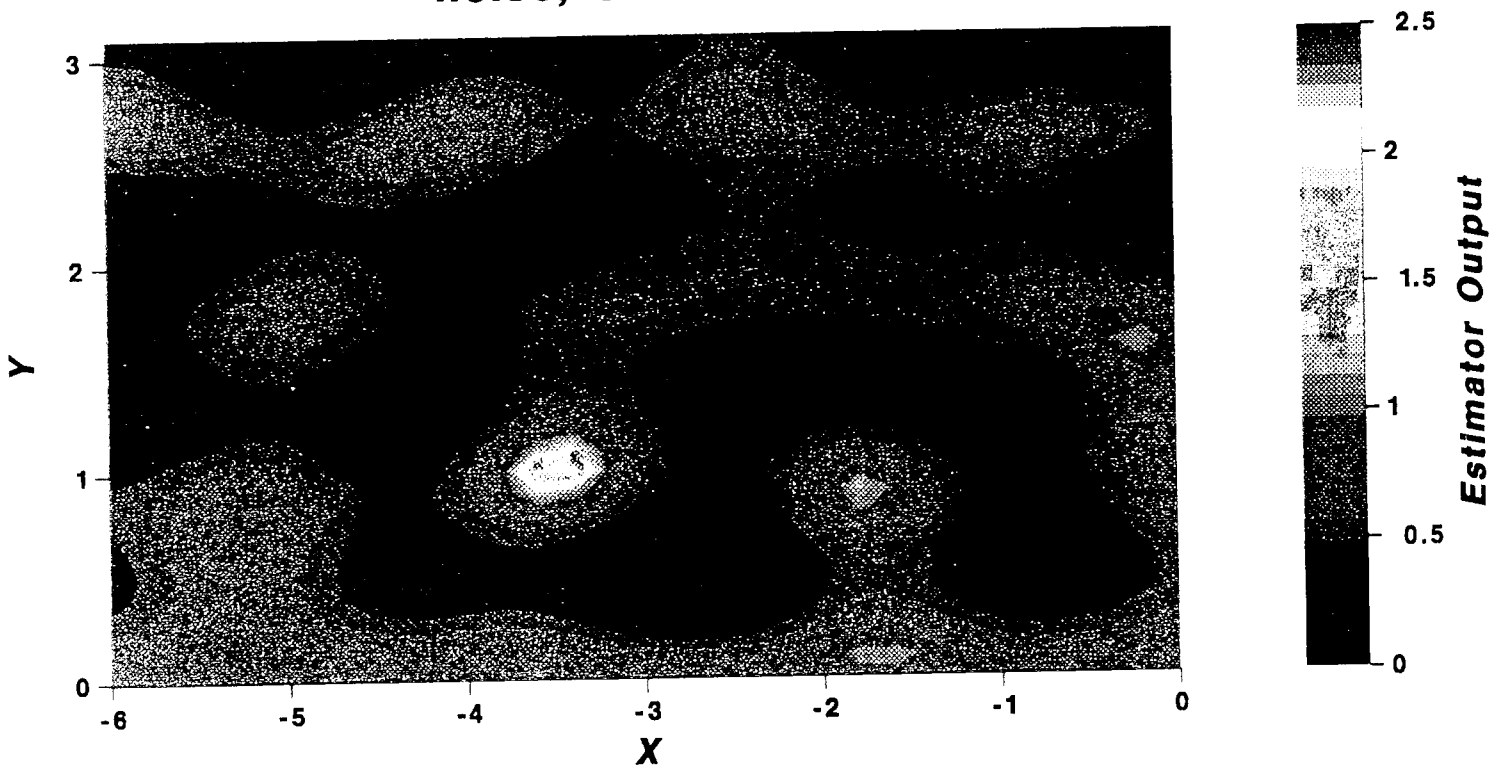

Figure 11: Estimator with filter threshold set at 0.65

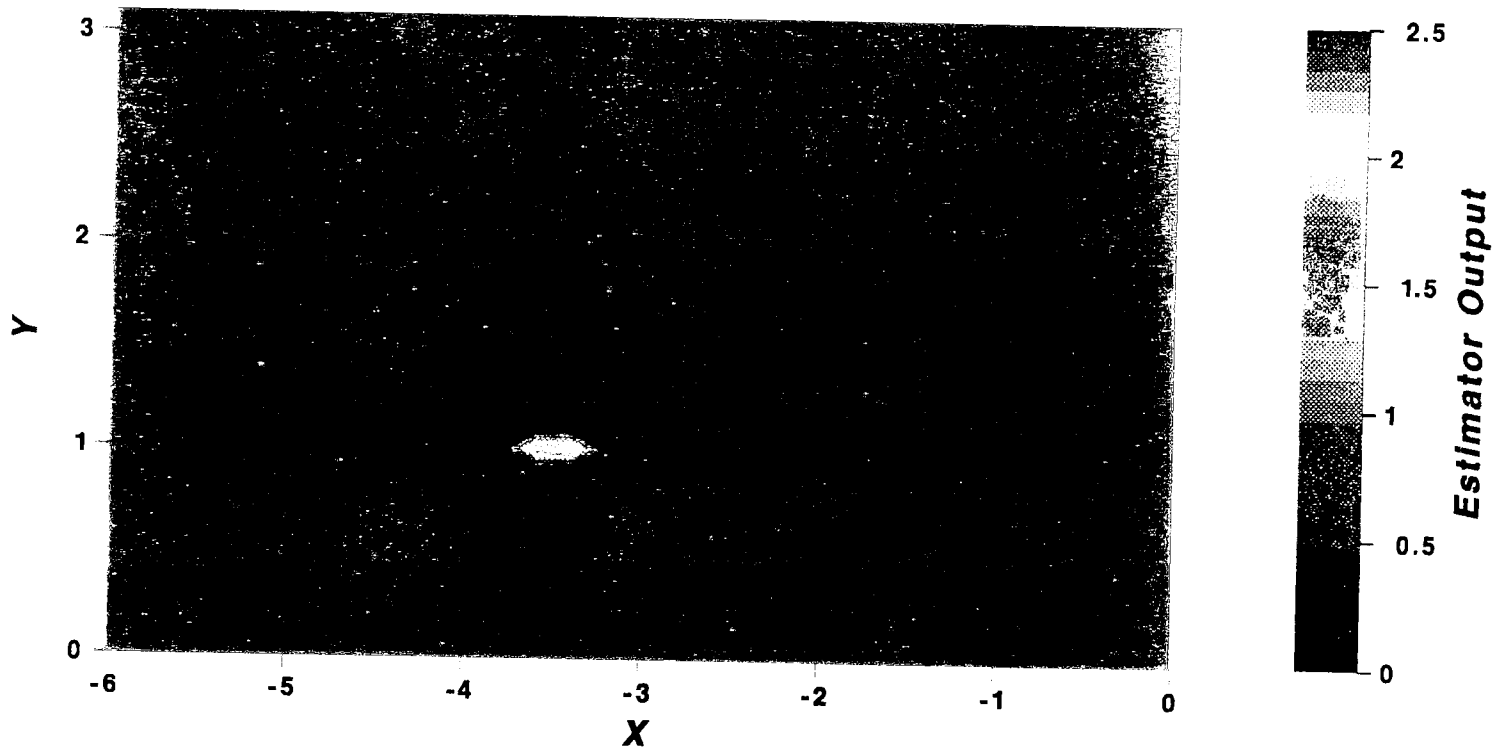

Figure 12: Estimator output when the calculated field is computed in the absence of the inclusion and hence mismatches the true field

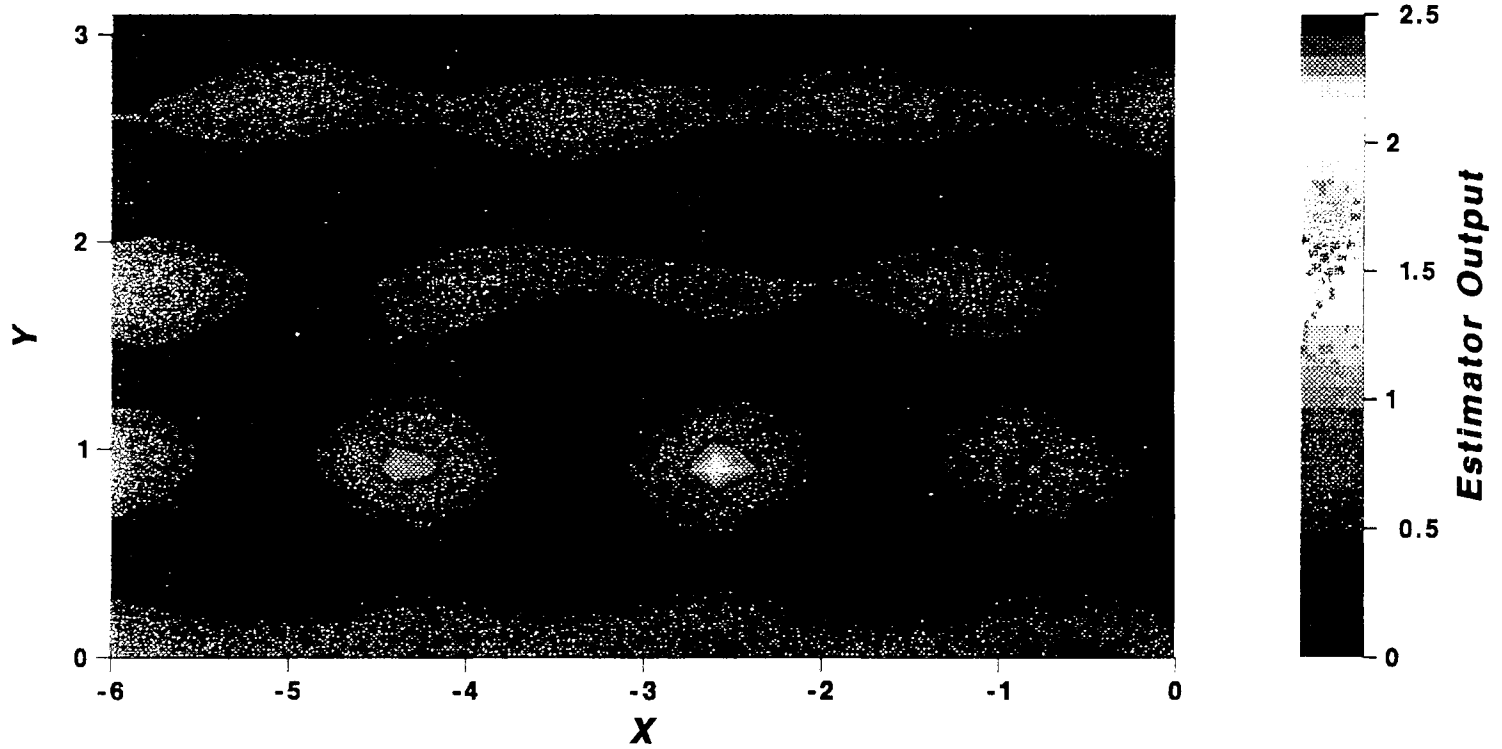

Figure 13: Same as Figure 12 with added Gaussian noise, S/N=10db, filter threshold set at .65

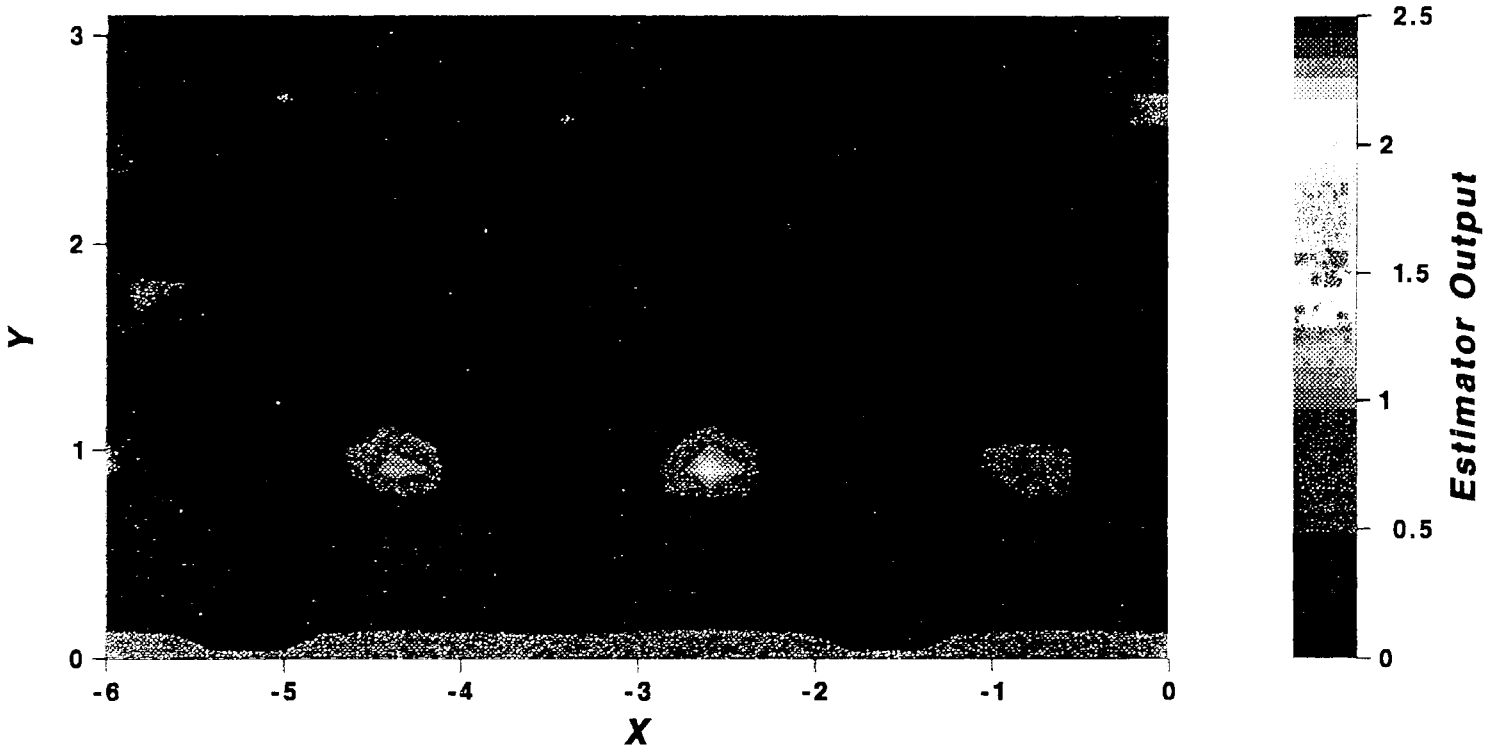

Recent IMA Preprints

#	Author/s	Title
892	**E.G. Kalnins, Willard Miller, Jr. and Sanchita Mukherjee**	Models of q-algebra representations: the group of plane motions
893	**T.R. Hoffend Jr. and R.K. Kaul**	Relativistic theory of superpotentials for a nonhomogeneous, spatially isotropic medium
894	**Reinhold von Schwerin**	Two metal deposition on a microdisk electrode
895	**Vladimir I. Oliker and Nina N. Uraltseva**	Evolution of nonparametric surfaces with speed depending on curvature, III. Some remarks on mean curvature and anisotropic flows
896	**Wayne Barrett, Charles R. Johnson, Raphael Loewy and Tamir Shalom**	Rank incrementation via diagonal perturbations
898	**Mingxiang Chen, Xu-Yan Chen and Jack K. Hale**	Structural stability for time-periodic one-dimensional parabolic equations
899	**Hong-Ming Yin**	Global solutions of Maxwell's equations in an electromagnetic field with the temperature-dependent electrical conductivity
900	**Robert Grone, Russell Merris and William Watkins**	Laplacian unimodular equivalence of graphs
901	**Miroslav Fiedler**	Structure-ranks of matrices
902	**Miroslav Fiedler**	An estimate for the nonstochastic eigenvalues of doubly stochastic matrices
903	**Miroslav Fiedler**	Remarks on eigenvalues of Hankel matrices
904	**Charles R. Johnson, D.D. Olesky, Michael Tsatsomeros and P. van den Driessche**	Spectra with positive elementary symmetric functions
905	**Pierre-Alain Gremaud**	Thermal contraction as a free boundary problem
906	**K.L. Cooke, Janos Turi and Gregg Turner**	Stabilization of hybrid systems in the presence of feedback delays
907	**Robert P. Gilbert and Yongzhi Xu**	A numerical transmutation approach for underwater sound propagation
908	**LeRoy B. Beasley, Richard A. Brualdi and Bryan L. Shader**	Combinatorial orthogonality
909	**Richard A. Brualdi and Bryan L. Shader**	Strong hall matrices
910	**Håkan Wennerström and David M. Anderson**	Difference versus Gaussian curvature energies; monolayer versus bilayer curvature energies applications to vesicle stability
911	**Shmuel Friedland**	Eigenvalues of almost skew symmetric matrices and tournament matrices
912	**Avner Friedman, Bei Hu and J.L. Velazquez**	A Free Boundary Problem Modeling Loop Dislocations in Crystals
913	**Ezio Venturino**	The Influence of Diseases on Lotka-Volterra Systems
914	**Steve Kirkland and Bryan L. Shader**	On Multipartite Tournament Matrices with Constant Team Size
915	**Richard A. Brualdi and Jennifer J.Q. Massey**	More on Structure-Ranks of Matrices
916	**Douglas B. Meade**	Qualitative Analysis of an Epidemic Model with Directed Dispersion
917	**Kazuo Murota**	Mixed Matrices Irreducibility and Decomposition
918	**Richard A. Brualdi and Jennifer J.Q. Massey**	Some Applications of Elementary Linear Algebra in Combinations
919	**Carl D. Meyer**	Sensitivity of Markov Chains
920	**Hong-Ming Yin**	Weak and Classical Solutions of Some Nonlinear Volterra Integrodifferential Equations
921	**B. Leinkuhler and A. Ruehli**	Exploiting Symmetry and Regularity in Waveform Relaxation Convergence Estimation
922	**Xinfu Chen and Charles M. Elliott**	Asymptotics for a Parabolic Double Obstacle Problem
923	**Yongzhi Xu and Yi Yan**	An Approximate Boundary Integral Method for Acoustic Scattering in Shallow Oceans
924	**Yongzhi Xu and Yi Yan**	Source Localization Processing in Perturbed Waveguides
925	**Kenneth L. Cooke and Janos Turi**	Stability, Instability in Delay Equations Modeling Human Respiration
926	**F. Bethuel, H. Brezis, B.D. Coleman and F. Hélein**	Bifurcation Analysis of Minimizing Harmonic Maps Describing the Equilibrium of Nematic Phases Between Cylinders
927	**Frank W. Elliott, Jr.**	Signed Random Measures: Stochastic Order and Kolmogorov Consistency Conditions
928	**D.A. Gregory, S.J. Kirkland and B.L. Shader**	Pick's Inequality and Tournaments
929	**J.W. Demmel, N.J. Higham and R.S. Schreiber**	Block LU Factorization
930	**Victor A. Galaktionov and Juan L. Vazquez**	Regional Blow-Up in a Semilinear Heat Equation with Convergence to a Hamilton-Jacobi Equation
931	**Bryan L. Shader**	Convertible, Nearly Decomposable and Nearly Reducible Matrices
932	**Dianne P. O'Leary**	Iterative Methods for Finding the Stationary Vector for Markov Chains
933	**Nicholas J. Higham**	Perturbation theory and backward error for $AX - XB = C$
934	**Z. Strakos and A. Greenbaum**	Open questions in the convergence analysis of the lanczos process for the real symmetric eigenvalue problem
935	**Zhaojun Bai**	Error analysis of the lanczos algorithm for the nonsymmetric eigenvalue problem
936	**Pierre-Alain Gremaud**	On an elliptic-parabolic problem related to phase transitions in shape memory alloys
937	**Bojan Mohar and Neil Robertson**	Disjoint essential circuits in toroidal maps

939 **Bojan Mohar and Svatopluk Poljak** Eigenvalues in combinatorial optimization
940 **Richard A. Brualdi, Keith L. Chavey and Bryan L. Shader**, Conditional sign-solvability
941 **Roger Fosdick and Ying Zhang**, The torsion problem for a nonconvex stored energy function
942 **René Ferland and Gaston Giroux**, An unbounded mean-field intensity model: Propagation of the convergence of the empirical laws and compactness of the fluctuations
943 **Wei-Ming Ni and Izumi Takagi**, Spike-layers in semilinear elliptic singular Perturbation Problems
944 **Henk A. Van der Vorst and Gerard G.L. Sleijpen**, The effect of incomplete decomposition preconditioning on the convergence of conjugate gradients
945 **S.P. Hastings and L.A. Peletier**, On the decay of turbulent bursts
946 **Apostolos Hadjidimos and Robert J. Plemmons**, Analysis of p-cyclic iterations for Markov chains
947 **ÅBjörck, H. Park and L. Eldén**, Accurate downdating of least squares solutions
948 **E.G. Kalnins, Willard Miller, Jr. and G.C. Williams**, Recent advances in the use of separation of variables methods in general relativity
949 **G.W. Stewart**, On the perturbation of LU, Cholesky and QR factorizations
950 **G.W. Stewart**, Gaussian elimination, perturbation theory and Markov chains
951 **G.W. Stewart**, On a new way of solving the linear equations that arise in the method of least squares
952 **G.W. Stewart**, On the early history of the singular value decomposition
953 **G.W. STewart**, On the perturbation of Markov chains with nearly transient states
954 **Umberto Mosco**, Composite media and asymptotic dirichlet forms
955 **Walter F. Mascarenhas**, The structure of the eigenvectors of sparse matrices
956 **Walter F. Mascarenhas**, A note on Jacobi being more accurate than QR
957 **Raymond H. Chan, James G. Nagy and Robert J. Plemmons**, FFT-based preconditioners for Toeplitz-Block least squares problems
958 **Zhaojun Bai**, The CSD, GSVD, their applications and computations
959 **D.A. Gregory, S.J. Kirkland and N.J. Pullman**, A bound on the exponent of a primitive matrix using Boolean rank
960 **Richard A. Brualdi, Shmuel Friedland and Alex Pothen**, Sparse bases, elementary vectors and nonzero minors of compound matrices
961 **J.W. Demmel**, Open problems in numerical linear algebra
962 **James W. Demmel and William Gragg**, On computing accurate singular values and eigenvalues of acyclic matrices
963 **James W. Demmel**, The inherent inaccuracy of implicit tridiagonal QR
964 **J.J.L. Velázquez**, Estimates on the $(N-1)$-dimensional Hausdorff measure of the blow-up set for a semilinear heat equation
965 **David C. Dobson**, Optimal design of periodic antireflective structures for the Helmholtz equation
966 **C.J. van Duijn and Joseph D. Fehribach**, Analysis of planar model for the molten carbonate fuel cell
967 **Yongzhi Xu, T. Craig Poling and Trent Brundage**, Source localization in a waveguide with unknown large inclusions
968 **J.J.L. Velázquez**, Higher dimensional blow up for semilinear parabolic equations
969 **E.G. Kalnins and Willard Miller, Jr.**, Separable coordinates, integrability and the Niven equations
970 **John M. Chadam and Hong-Ming Yin**, A diffusion equation with localized chemical reactions
971 **A. Greenbaum and L. Gurvits**, Max-min properties of matrix factor norms
972 **Bei Hu**, A free boundary problem arising in smoulder combustion
973 **C.M. Elliott and A.M. Stuart**, The global dynamics of discrete semilinear parabolic equations
974 **Avner Friedman and Jianhua Zhang**, Swelling of a rubber ball in the presence of good solvent
975 **Avner Friedman and Juan J.L. Velázquez**, A time-dependence free boundary problem modeling the visual image in electrophotography
976 **Richard A. Brualdi, Hyung Chan Jung and William T. Trotter, Jr.**, On the poset of all posets on n elements
977 **Ricardo D. Fierro and James R. Bunch**, Multicollinearity and total least squares
978 **Adam W. Bojanczyk, James G. Nagy and Robert J. Plemmons**, Row householder transformations for rank-k Cholesky inverse modifications
979 **Chaocheng Huang**, An age-dependent population model with nonlinear diffusion in R^n
980 **Emad Fatemi and Faroukh Odeh**, Upwind finite difference solution of Boltzmann equation applied to electron transport in semiconductor devices
981 **Esmond G. Ng and Barry W. Peyton**, A tight and explicit representation of Q in sparse QR factorization
982 **Robert J. Plemmons**, A proposal for FFT-based fast recursive least-squares
983 **Anne Greenbaum and Zdenek Strakos**, Matrices that generate the same Krylov residual spaces
984 **Alan Edelman and G.W. Stewart**, Scaling for orthogonality
985 **G.W. Stewart**, Note on a generalized sylvester equation
986 **G.W. Stewart**, Updating URV decompositions in parallel